

ISTITUTO NAZIONALE DI FISICA NUCLEARE
Laboratori Nazionali di Frascati

LNF-79/7(R)
22 Gennaio 1979

V. Bellini, E. De Sanctis, P. Di Giacomo, V. Emma, S. Gentile,
C. Guaraldo, S. Lo Nigro, V. Lucherini, C. Milone, G. S. Pap-
palardo and A. R. Reolon: FISSION INDUCED IN HEAVY
ELEMENTS BY THE LEALE MONOCHROMATIC PHOTON
BEAM OF FRASCATI.

LNF-79/7(R)
22 Gennaio 1979

V. Bellini^(x), E. De Sanctis, P. Di Giacomo, V. Emma^(x), S. Gentile, C. Guaraldo, S. Lo Nigro^(x), V. Lucherini, C. Milone^(x), G.S. Pappalardo^(x) and A.R. Reolon:
FISSION INDUCED IN HEAVY ELEMENTS BY THE LEALE MONOCHROMATIC PHOTON BEAM
OF FRASCATI.

1. - INTRODUCTION.

The photofission of heavy elements at photon energies $k \geq 100$ MeV has been largely studied in several laboratories⁽¹⁻¹⁷⁾ only by bremsstrahlung photon beams because of the lack of suitable powerful monochromatic gamma sources with variable energy.

The photofission yields per equivalent quantum $g(k_m)$ are measured for several values of the maximum energy k_m of the bremsstrahlung spectrum. The fission cross-section $f(k)$ is deduced from the experimental yields by solving the integral equation of the process (Volterra linear equation) in the form

$$g(k_m) = \int_0^{k_m} \mathcal{N}(k, k_m) f(k) dk \quad (1)$$

where $\mathcal{N}(k, k_m)$ is the number of photons per unit k interval.

Several numerical methods⁽¹⁸⁻²³⁾ have been developed in order to solve equations of the type (1), that, as it is well known, are particularly "unstable". Considerable difficulties are found if the kernel $\mathcal{N}(k, k_m)$ has a very weak dependence on the energy⁽²⁰⁾, as in the case of measurements made with bremsstrahlung beam from an amorphous target. This could partially explain the discrepancies among the $f(k)$ behaviours reported in the literature^(2, 3, 5, 6, 8-17).

In previous papers⁽²⁴⁻²⁶⁾ an improvement in fission measurements was obtained by using the quasi-monochromatic photon beam from the Frascati electronsynchrotron by coherent bremsstrahlung of 1000 MeV electrons striking a diamond single crystal. This photon beam was characterized by a "quasi-monoenergetic" main peak lying on a continuous spectrum⁽²⁷⁾. The experimental yields, for $k_m = 1000$ MeV fixed energy, resulted to depend noticeable on the energy k_j of the photon main peak. The accurate knowledge of the used photon spectra and the application of an appropriate unfolding method to the experimental data permitted to deduce^(25, 26) the photofission

(x) - INFN - Sezione di Catania.

sion cross-section with higher reliability than the $f(k)$ behaviour obtained by other authors by bremsstrahlung photon beams.

The experimental yields measured for 9 elements with $73 \leq Z \leq 92$ resulted consistent with cross-sections that clearly show a resonance centred at photon energy of about 340 MeV in a very good agreement with the energy of the first baryon resonance in the pion photoproduction. The energy dependence of the obtained cross-sections was adequately explained^(26, 28) by assuming a photomesonic mechanism of the fission process with a nuclear fissility increasing with photon energy at least up to 500 MeV.

The experiment with the coherent photon beam was performed by changing the energy k_j of the main photon peak in the range from 220 MeV to 550 MeV; thus the results are reliable in this energy region. For experimental reasons it was not possible to work at energies $k_j < 220$ MeV.

The opportunity to extend the photofission measurements at lower energies, with particular care for the region near the photomesonic threshold, has been offered by the monochromatic photon beam from annihilation of positrons on hydrogen realised at the LEALE Laboratory of Frascati⁽²⁹⁾. This photon beam shows a monoenergetic peak at the correct annihilation energy with a bremsstrahlung continuous tail.

The main characteristic of the photon source are described in Sect. 2.

The energy of the monochromatic photon peak can range from 100 MeV to 300 MeV.

This enable us to perform measurements in an energy range where the accurate knowledge of the photofission cross-section could permit to deduce informations on the energy dependence of the nuclear fissility at energies where both the role of nucleon clusters (quasi-deuteron model) and of single nucleons (photomesonic model) are relevant in the photon absorption by the nucleus.

In order to estimate the cross-section with good reliability it is necessary to know exactly the shape of the used photon spectra. Photon energy spectrum measurements are performed by a magnetic pairs spectrometer - described in Sect. 3 - that enable to measure on-line the spectrum of the photon beam during the irradiation of the photofission samples.

The results of the search for the experimental conditions at which it is advantageous to use the annihilation photon beam in order to perform fission experiments, are reported in Sect. 4.

The behaviour of the photofission yields has been calculated taking into account the improving of the annihilation to bremsstrahlung ratio N_A/N_B as a function of the collection angle of the photon beam. Meanwhile intensity and energy resolution of the photon peak decrease. For this reason we looked for a compromision between a large value of the ratio N_A/N_B and a suitable intensity of the photon beam in order to have reasonable exposure times.

The experimental technique we used to detect the fission fragments is reported in Sect. 5.

2. - PHOTON BEAM.

The monochromatic photon beam is obtained by positrons annihilation on an hydrogen target, 0.011 radiation lengths thick. The absolute value of the positrons current on the target can be measured by a Faraday cup (used also as beam catcher) put in the focal plane of a damping magnet, after the annihilation target. The expected features of the photon beam have been evaluated by taking into account the positron beam characteristics, the multiple scattering and the energy loss in the target⁽³⁰⁾.

In Fig. 1 the results of the calculation performed for a 0.011 radiation lengths thick hydrogen target, at two different angular collection conditions, in the energy range 100 - 300 MeV, are given. The dashed curves give the number of annihilation photon per incident positron. The solid lines give the number of annihilation photons per second. The dotted curves give the FWHM energy resolution of the annihilation peak.

Photon yield measurements are performed with the aid of a Wilson type quantameter modified

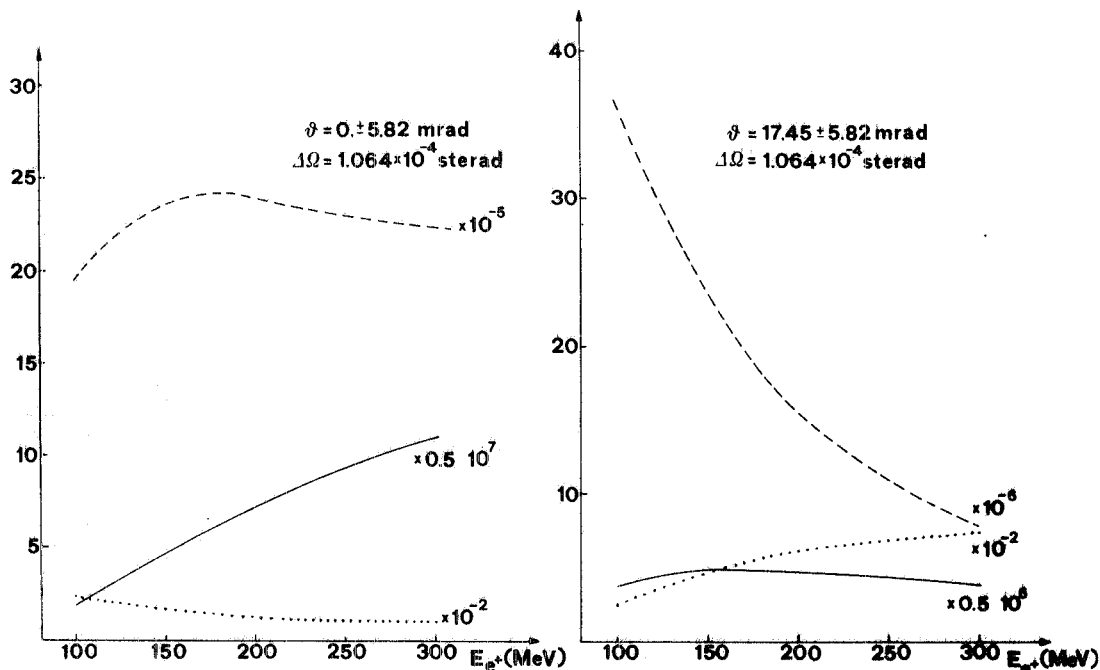


FIG. 1 - Photon beam features for 0.011 radiation lengths hydrogen target at a) $0.0 \pm 5.8 \text{ mrad}$ and b) $17.5 \pm 5.8 \text{ mrad}$ photon collection angle θ_γ . The dashed lines give the number of photons per incident position. The solid lines give the number of annihilation photons per second (Cu converter, 100 p.p.s. repetition rate). The dotted lines give the FWHM annihilation peak resolution.

in the integration system according to Komar suggestions⁽³¹⁾, in order to obtain a constant sensitivity in the energy range 5 MeV \pm 5 GeV.

By two bending magnets which give a vertical deflection⁽³²⁾ the positrons direction may be changed by 0° up to 1.5° with respect to the one of the photon collection.

As it is known⁽³³⁾ (see Fig. 2), the increasing of the collection angle θ_γ of the photon beam respect to the positron one, improves the annihilation to bremsstrahlung ratio. Meanwhile, intensity and energy resolution strongly decrease with angle. In Fig. 2 the behaviour of the ratio $R = N_A/N_B$ (N_A = number of annihilation photons, N_B = number of bremsstrahlung photons, with energy above 5 MeV) versus the mean photon collection angle, at a fixed collimation and for two positron energies, is reported.

3. - PHOTON ENERGY SPECTRUM MEASUREMENTS.

A rectangular flat pole C-type magnet already existing in Frascati Laboratories (dimensions $40 \times 90 \text{ cm}^2$, gap 15 cm; PS in Fig. 3) is used as an on-line pairs spectrometer^(34, 35). The electron positron pairs are deflected at $\sim 110^\circ$ and are detected by two multiwires proportional chambers (useful areas $26 \times 13 \text{ cm}^2$). The spectrometer characteristics are: momentum acceptance $\sim 14\%$; resolution better than 0.17%; energy dispersion $\sim 0.77 \text{ MeV/cm}$. The overall distance

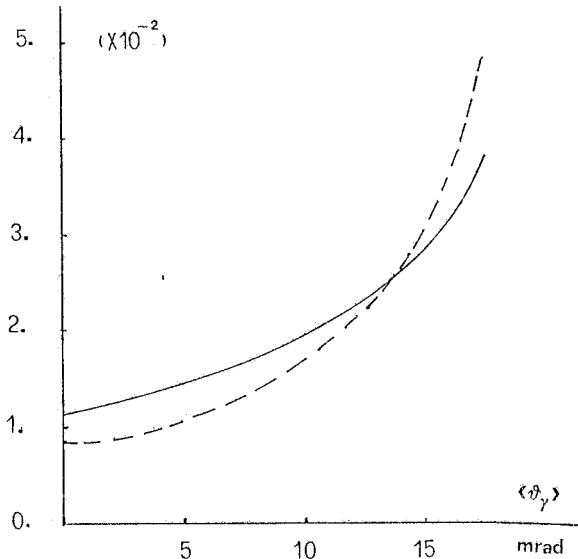


FIG. 2 - Behaviour of the ratio $R = N_A/N_B$ (N_A = number of annihilation photons, N_B = number of bremsstrahlung photons, with energy above 5 MeV) versus $\langle \theta_\gamma \rangle$ at a fixed collimation (± 4 mrad) and for two position energies ($E_{e^+} = 150.51$ MeV full line; $E_{e^+} = 200.51$ MeV, dashed line).

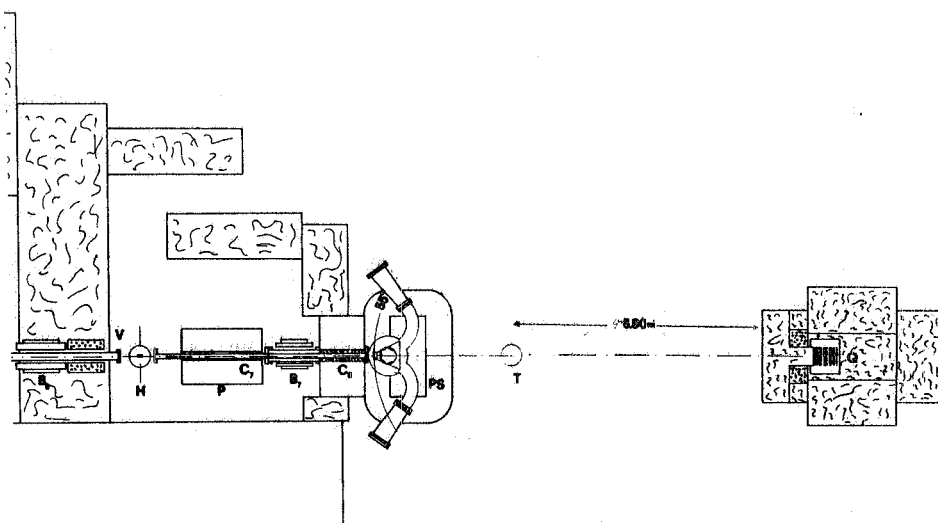


FIG. 3 - Photon beam layout. B_6B_7 bending magnets; H hydrogen target; D damping magnet; C_7C_8 collimators; PS pairs spectrometer; T experimental; Q quantum meter.

between the conversion targets and the wires chambers is under vacuum. In Fig. 4 a picture of the vacuum chamber is shown. Five aluminum targets can be inserted on the photon beam: three rectangular shaped (1×55 , 3×55 , 10×55 mm 2 , respectively) 0.005 mm thick; the fourth and the fifth, circular, 55 mm diameter, 0.005 and 0.01 mm thick, respectively. A target out position is also available.

The counting rate expected with an aluminum converter $1 \cdot 10^{-4}$ radiation lengths thick, for photon energies 295 ± 300 MeV and photon yields $5 \cdot 10^4$ γ/sec is about 40 counts/sec.

At present, in both arms of the spectrometer electrons (positrons) are detected by a four plastic scintillators hodoscope $E_1 + E_4$ ($P_1 + P_4$) (dimensions $10 \times 1 \times 2$ cm 3) followed by a fifth counter $E_5(P_5)$ (dimensions 10×0.5 cm 3). In Fig. 5 the block diagram of the electronics is reported.

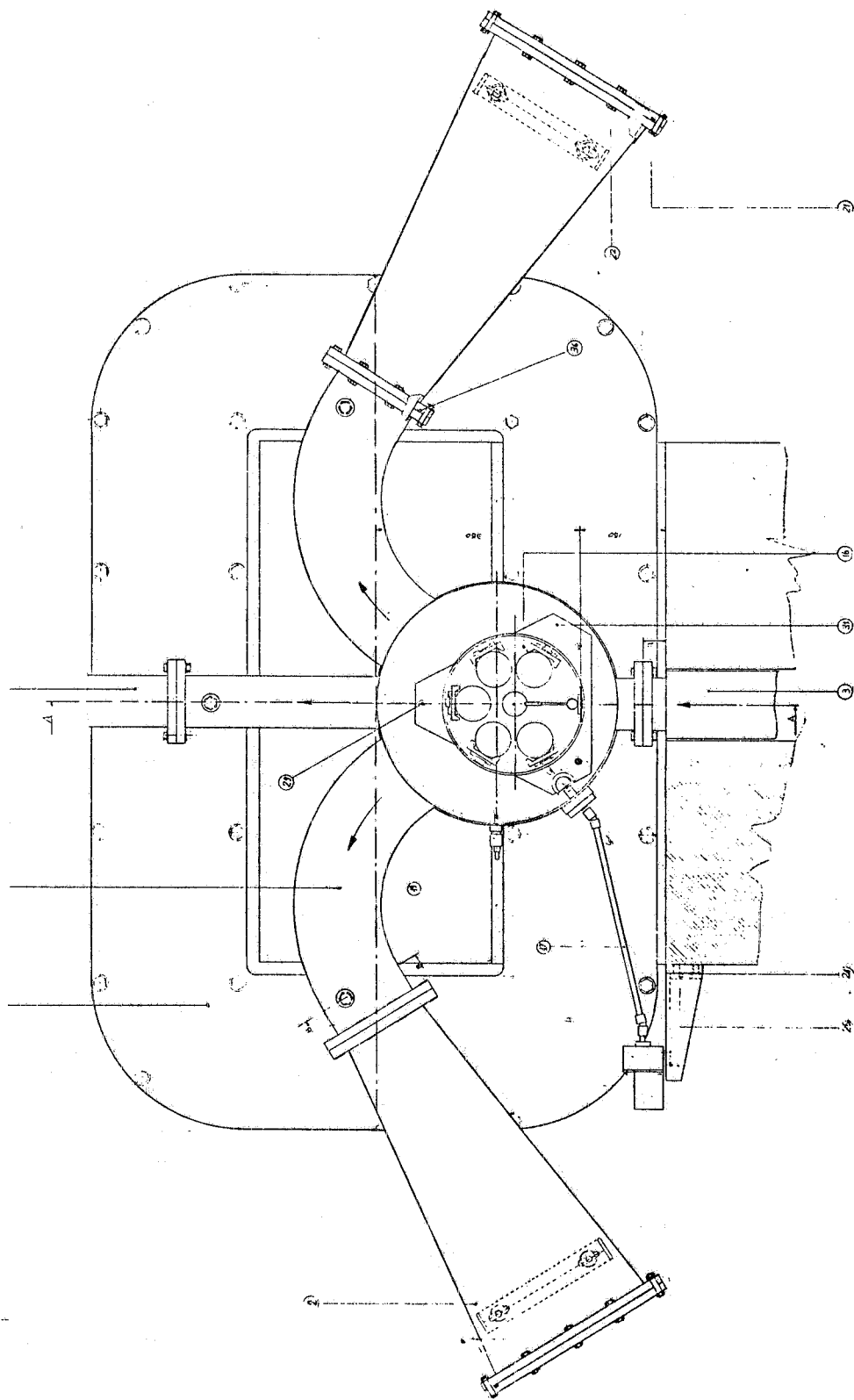


FIG. 4 - Pairs spectrometer vacuum chamber.

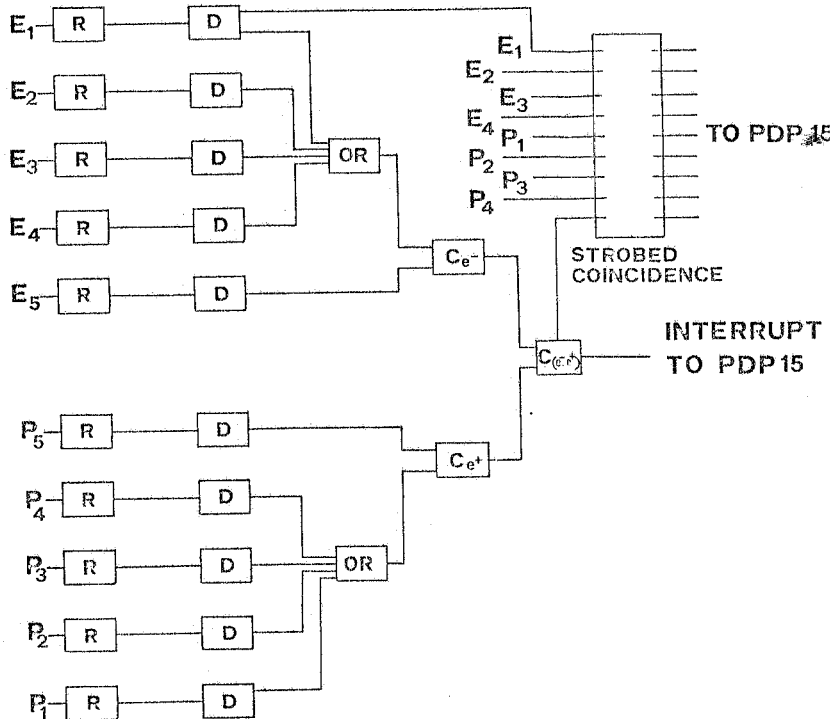


FIG. 5 - Block diagram of the electronics for the detection system in the pairs spectrometer.

Signals from the various counters are transferred to a PDP 15/40 computer, which gives on a scope an on-line energy spectrum of the photon beam.

4. - PHOTOFISSION MEASUREMENTS.

In photoreaction experiments the optimum condition is represented by a monochromatic photon beam, as the experimental yields measured at different energies of the photon peak directly give the cross-section without solving the integral equation of the process.

By using a quasi monochromatic photon beam, as that described in Sect. 2, a sensible improvement respect to a bremsstrahlung photon beam is obtained if the contribution to the studied photoreaction due to the monochromatic peak is relevant compared to the contribution due to the continuous bremsstrahlung tail.

In order to investigate the suitability of the use of a photon beam from annihilation for photofission experiments we calculated the behaviour of the yields expected starting from an assumed $f(k)$ cross-section and making different hypothesis on the value of the ratio N_A/N_B . This ratio, as previously said, increases by increasing the collection angle θ_γ of the photon beam.

In the calculation the studied nuclei were divided into two groups:

- nuclei with fission threshold at energy below the giant resonance ($Z \gg 90$);
- nuclei with fission threshold at energy above the giant resonance, but below the threshold of pion photoproduction ($70 \leq Z \leq 83$).

The yields were calculated by folding the eq. (1) with the kernel $\mathcal{N}(k, k_m)$ properly evaluated taking into account various experimental condition of the photon spectrum.

At present, only preliminary measurements were performed with the magnetic pairs spectrometer. The photon spectrum from annihilation of positrons was calculated starting from the electromagnetic cross-section and taking into account positron beam characteristics, multiple scattering and energy loss in the target and in the crossed media.

The photon spectra were estimated for 11 positron energies, spaced 20 MeV from 100 MeV to 300 MeV and two different θ_γ , 0 ± 5 mrad and 17.5 ± 5 mrad, respectively.

The calculations were not extended at angles higher than 17.5 mrad, due to the strong decreasing of the photon intensity and to the low fission cross-sections expected in the energy region considered.

In order to solve the integral (1), the kernel $\mathcal{N}(k, k_m)$ was calculated at equally spaced values of k , with 5 MeV steps and correspondently we assumed a $f(k)$ cross-section, as we shall say later on.

The numerical integration was performed by means of the Simpson formula, assuming the energy of the incident positron as upper limit of the integral (1).

4. 1 - Nuclei with $Z \gg 90$.

In the case of photofission of $Z \gg 90$ nuclei, the contribution due to the dipole absorption of photons (giant resonance) is relevant because of the low fission threshold energy.

For our calculation we chose ^{238}U for which the $f(k)$ is known enough in literature⁽³⁶⁾ for $k \leq 100$ MeV.

In Fig. 6 the assumed $f(k)$ cross-section is reported. The dashed curve ($k \leq 100$ MeV) shows the behaviour deduced from the results of other authors⁽³⁶⁾, the continuous one ($k > 100$ MeV) represents the behaviour obtained by the coherent photon beam of Frascati⁽²⁶⁾.

The continuous curves reported in Fig. 7 are the results of the $g(k_m)$ yields expected at two different values of θ_γ . In the same figure the dashed curves represent the $g_B(k_m)$ yields calculated by considering only the contribution arising from the bremsstrahlung photons held in the spectra.

The comparison between the curves of Fig. 7 clearly indicates that the annihilation photon beam at $\theta_\gamma = 17.5$ mrad is more resolutive than the photon beam at $\theta_\gamma = 0$ mrad. In the last case, in fact, the contribution to the yields from the monochromatic photon peak is very small with respect to the one from the bremsstrahlung photons. The $g_B(k_m)$ contribution is certainly relevant in the Uranium photofission because of the high value of the cross-section at 10-20 MeV photon energies, as Fig. 6 shows, and of the large number of bremsstrahlung photons.

In Fig. 8 the values of the ratio $[g(k_m) - g_B(k_m)] / g(k_m)$ at two different angles θ_γ are reported. This ratio represents the contribution to the yields coming from the annihilation photon peak with respect to that from the whole spectrum.

The continuous curve, calculated with the spectrum at $\theta_\gamma = 17.5$ mrad, just shows the advantage that one reaches by using the photon beam with a higher ratio N_A/N_B .

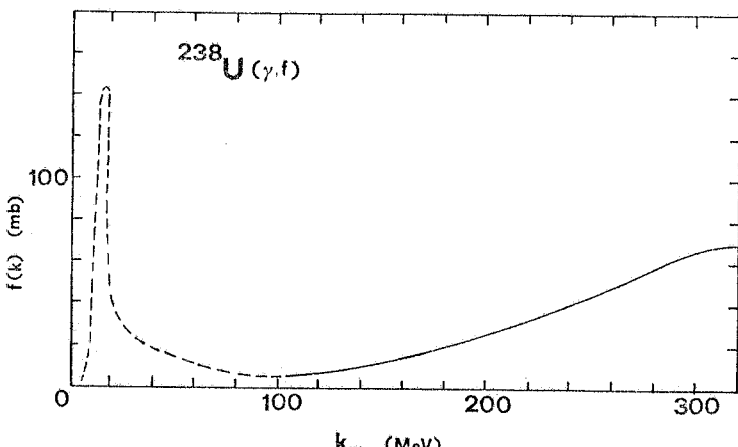


FIG. 6 - Photofission cross-section of ^{238}U versus the photon energy k_m of the annihilation peak. Dashed curve: behaviour deduced from literature. Continuous curve: behaviour obtained by Frascati coherent photon beam.

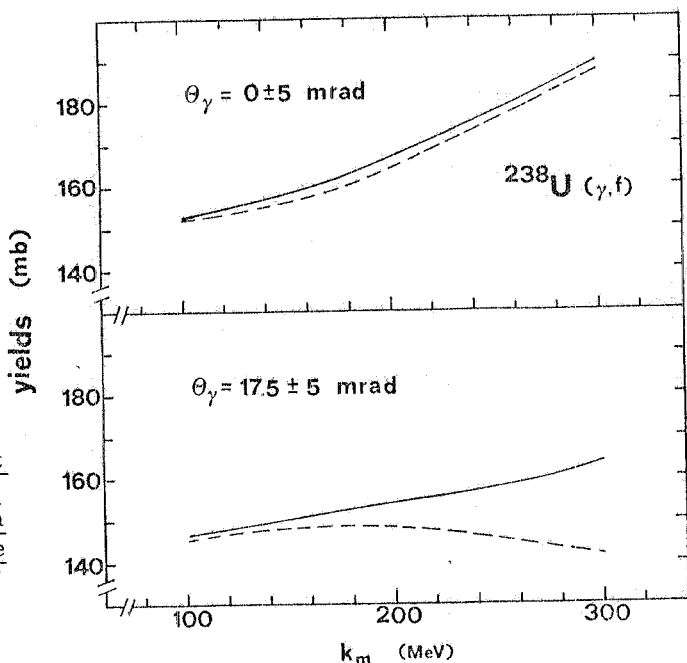


FIG. 7 - Photofission yields of ^{238}U calculated at two different angle θ_γ (continuous curves). The dashed lines represent the calculated yields $g_B(k_m)$ from the absorption of bremsstrahlung photons of the continuous tail of the spectra.

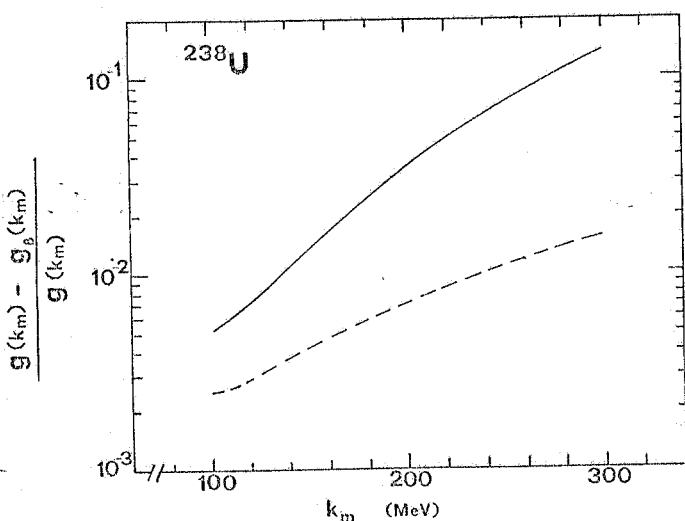


FIG. 8 - Values of the ratio $[g(k_m) - g_B(k_m)] / g(k_m)$ estimated for ^{238}U at two angles θ_γ . Dashed curve: $\theta_\gamma = 0 \pm 5$ mrad. Continuous curve: $\theta_\gamma = 17.5 \pm 5$ mrad.

4.2 - Nuclei with $Z \leq 83$.

For $Z \leq 83$ nuclei, the contribution due to the absorption of photons from the giant resonance is negligible because of the high fission threshold energy.

We performed the calculations on Bi by assuming the $f(k)$ behaviour obtained in the previous measurements (25).

As the data were in arbitrary units, we calculated the $f(k)$ values in barn by evaluating the total absorption cross-section on Bi at 340 MeV, following the procedure previously described (28), and assuming a constant fissility equal to 0.12, as suggested by Vartapetyan et al. (14). The obtained $f(k)$ cross-section is reported in Fig. 9. Taking into account the low photofission cross-section for $k < 80$ MeV, in folding the eq. (1) we neglected the value of the product $\mathcal{N}(k, k_m)f(k)$ for $k < 80$ MeV respect to its value averaged between 80 MeV and 300 MeV.

In Fig. 10 the $g(k_m)$ behaviours obtained with the photon spectra at $\theta_\gamma = 0$ mrad and $\theta_\gamma = 17.5$ mrad (continuous curves) are compared with the $g_B(k_m)$ values (dashed curves) expected by taking into account only the bremsstrahlung photon tail of the spectra.

The values of the ratio $[g(k_m) - g_B(k_m)] / g(k_m)$ at $\theta_\gamma = 0$ mrad (dashed curve) and $\theta_\gamma = 17.5$ mrad (continuous curve), respectively, are in Fig. 11.

FIG. 9 - Photofission cross-section of Bi as a function of the photon energy k_m of the annihilation peak.

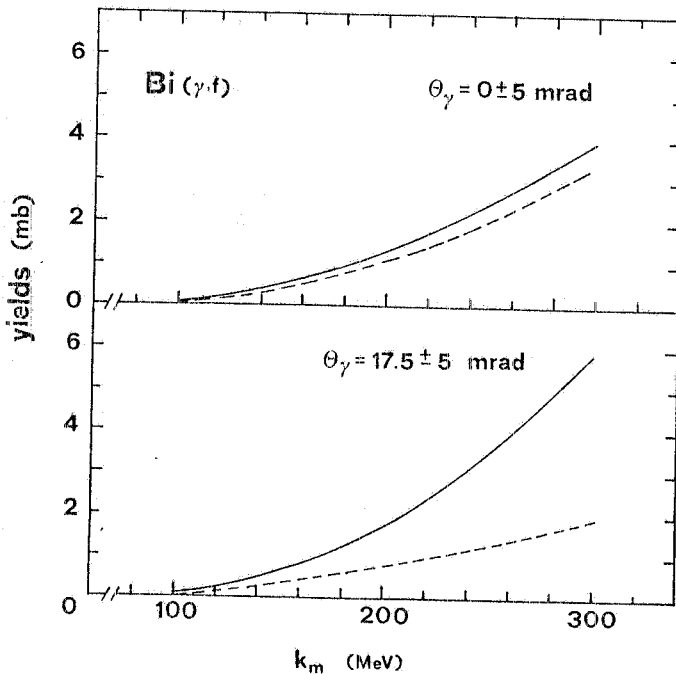
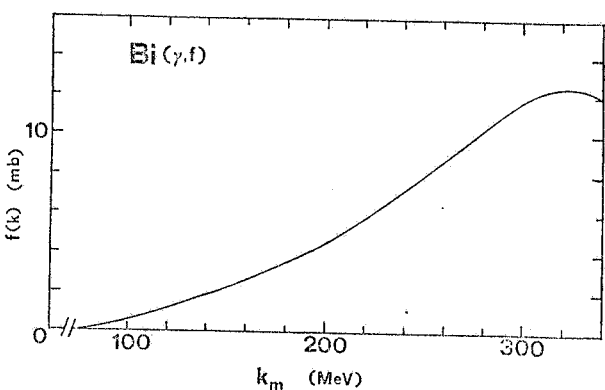
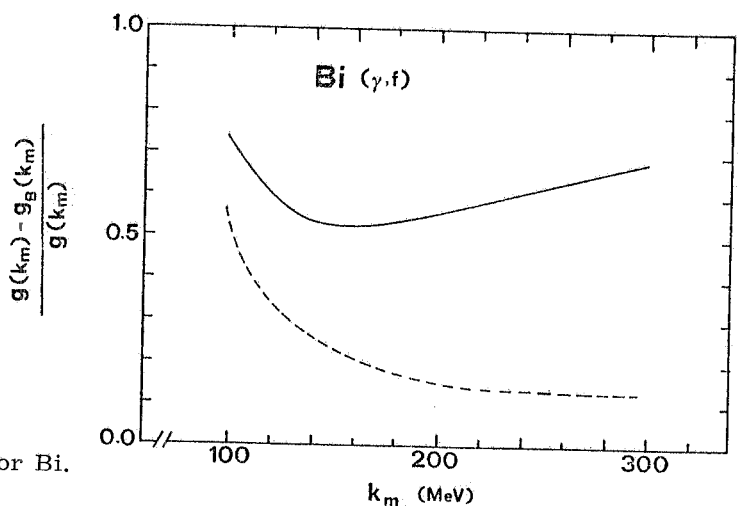


FIG. 10 - See caption to Fig. 7. Results for Bi.

FIG. 11 - See caption to Fig. 8. Results for Bi.



using
Non forward of the photon beam is clearly advantageous. At 17.5 mrad, in fact, the monochromatic part of the photon spectrum predominates in determining the fission yields, since in the case of Bi the contribution of the bremsstrahlung tail is small because of the low fission cross-section for $k < 80$ MeV.

As a consequence, the annihilation photons behave as a monochromatic beam.

5. - FISSION FRAGMENTS DETECTION.

In previous works (11, 24-26) we used glass sandwich detectors for fission cross-section measurements. This technique consists in putting a metal target of the sample between two glass plates. Each sandwich is exposed to the collimated photon beam which impinges orthogonally to the plates.

After the exposure, the glass plates are etched with a HF solution and the fission tracks, observed by an optical microscope, appear circular, as Fig. 12 shows.

The scanning system permits to discriminate the fission tracks from the damage of the glass plates due to the irradiation, especially in the case of large exposure doses for samples with very low fission cross-sections.

If the cross-section behaviour, and not its absolute value, is looked for, very thick targets ($0.2 \mu\text{m}$) are used. In this case, we are able to collect a sufficient number of fission tracks in reasonable exposure times.

In order to obtain the absolute values of the cross-sections thin targets of known thickness are requested. The sandwich detectors are prepared depositing by thermal evaporation a layer of the sample directly into the surface of one of the two glass plates. The plates are tightened together in order to ensure a complete surface contact. The thickness and the uniformity of each layer are measured by an optical interferometer and by the charged-particle backscattering technique. The first method, which requires an appropriate evaporation technique⁽³⁷⁾, allows only to measure the layer thickness with an experimental accuracy of $\pm 0.005 \mu\text{m}$. The second one, described in detail in ref. (36), gives directly the number of atoms per cm^2 of the sample with an experimental accuracy better than 5%.

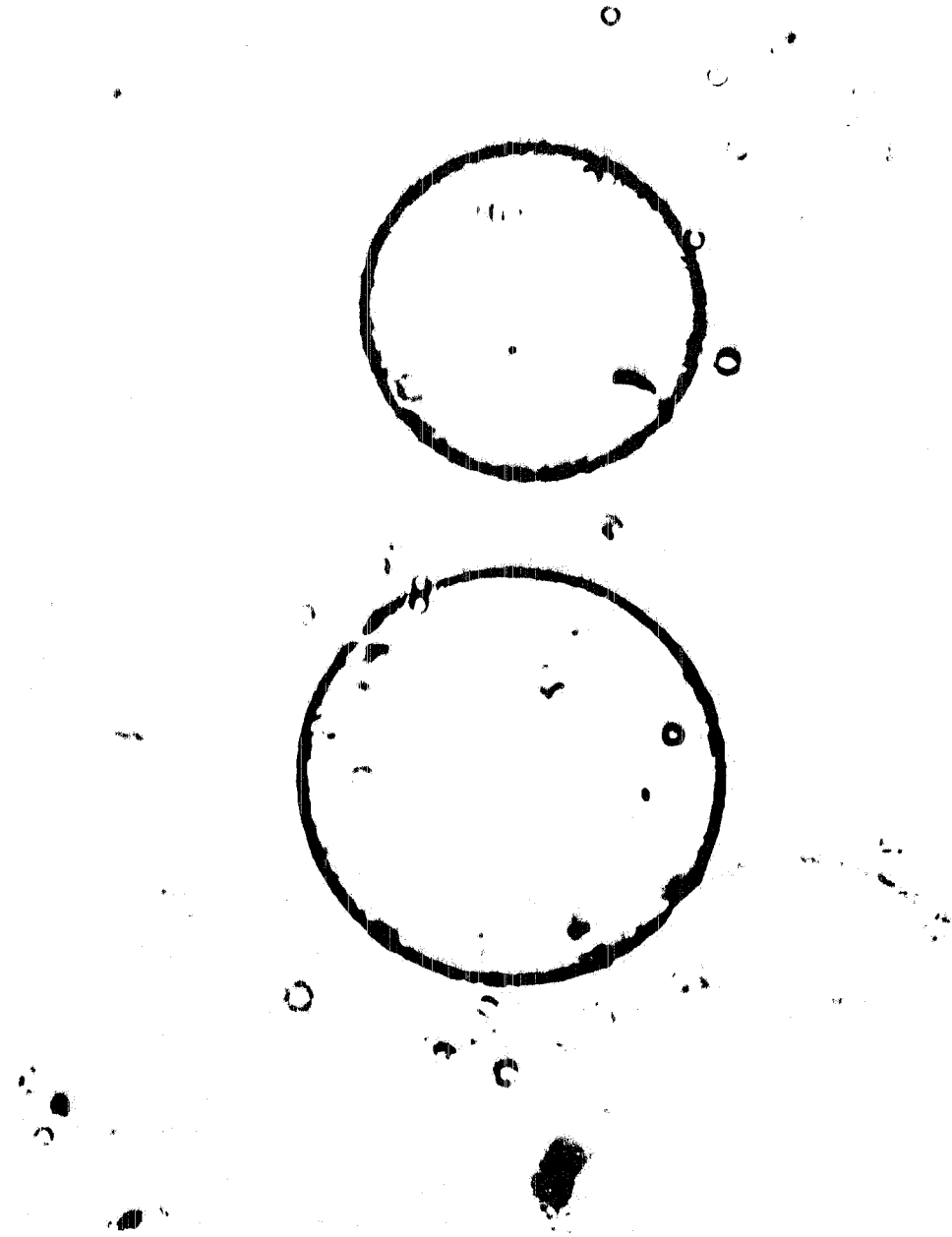


FIG. 12 - Etched tracks of fission fragments in glass detectors as observed by an optical microscope.

REFERENCES.

- (1) - G. Bernardini, R. Reitz and E. Segrè: Phys. Rev., 90, 573 (1953).
- (2) - J. A. Jungerman and H. M. Steiner: Phys. Rev., 106, 585 (1957).
- (3) - E. V. Minarik and V. A. Novikov: Sov. Phys. JETP, 5, 253 (1957).
- (4) - H. G. De Carvalho, A. Celano, G. Cortini, R. Rinzivillo and G. Ghigo: Nuovo Cimento, 19, 187 (1961).
- (5) - H. G. De Carvalho, G. Cortini, D. Del Giudice, G. Potenza, R. Rinzivillo and G. Ghigo: Nuovo Cimento, 32, 1717 (1964).
- (6) - F. Carbonara, H. G. De Carvalho, R. Rinzivillo, E. Sassi and G. P. Murtas: Nucl. Phys., 73, 385 (1965).
- (7) - Yu. N. Ranyuk and P. V. Sorokin: Sov. J. Nucl. Phys., 5, 26 (1967).
- (8) - A. V. Mitrofanova, Yu. N. Ranyuk and P. V. Sorokin: Sov. J. Phys., 6, 512 (1968).
- (9) - L. G. Moretto, R. C. Gatti, S. G. Thompson, J. T. Routti, J. H. Hesenberg, L. M. Middleman, M. R. Yearian and R. F. Hofstadter: Phys. Rev., 179, 1176 (1969).
- (10) - T. Methasiri: Nucl. Phys. 158A, 433 (1970).
- (11) - V. Emma, S. Lo Nigro and C. Milone: Nuovo Cimento Lett., 2, 117, 271 (1971).
- (12) - T. Methasiri and S. A. E. Johansson: Nucl. Phys., 167A, 97 (1971).
- (13) - Y. Wakuta: J. Phys. Soc. Jap., 31, 12 (1971).
- (14) - G. A. Vartapetyan, N. A. Demekhina, V. I. Kasilov, Yu. N. Ranyuk, P. V. Sorokin and A. G. Khudaverdyan: Sov. J. Phys., 14, 37 (1972).
- (15) - I. Kroon and B. Forkman: Nucl. Phys., 179A, 141 (1972).
- (16) - G. Andersson, I. Blomqvist, B. Forkman, G. G. Jönsson, A. Järund, I. Kroon, K. Lindgren and B. Schroder: Nucl. Phys. 197, 44 (1972).
- (17) - P. David, J. Debrus, U. Kim, G. Kumbartzki, H. Mommsen, W. Soyez, K. H. Speidel and G. Stein: Nucl. Phys., 197A, 163 (1972).
- (18) - L. Katz and A. G. W. Cameron: Can. Journ. Phys., 29, 518 (1951).
- (19) - A. S. Penfold and J. E. Leiss: Phys. Rev., 114, 1332 (1959).
- (20) - D. L. Phillips: J. Assoc. Comput. Mach., 9, 84 (1962).
- (21) - S. Twomey: J. Assoc. Comput. Mach., 10, 97 (1963).
- (22) - B. C. Cook: Nucl. Instr. 24, 256 (1963).
- (23) - V. F. Turchin, V. P. Kozlov and M. S. Malkevich: Sov. Phys. USPEKI, 13, 681 (1971).
- (24) - G. Bologna, V. Emma, A. S. Figueira, S. Lo Nigro and C. Milone: Phys. Lett., 52B, 192 (1974).
- (25) - G. Bologna, V. Bellini, V. Emma, A. S. Figueira, S. Lo Nigro, C. Milone and G. S. Pappalardo: Nuovo Cimento, 35A, 91 (1976).
- (26) - V. Bellini, V. Emma, A. S. Figueira, S. Lo Nigro, C. Milone, G. S. Pappalardo, and G. Bologna: Nuovo Cimento (1978) in press.
- (27) - G. Bologna: Nuovo Cimento, 49A, 756 (1967).
- (28) - V. Bellini, S. Lo Nigro and G. S. Pappalardo: Nuovo Cimento Lett. 19, 611 (1977).
- (29) - G. P. Capitani, E. De Sanctis, G. Guaraldo, R. Ricco, M. Sanzone, R. Scrimaglio, and A. Zucchiatti: Frascati Report LNF-77/45 (1977).
- (30) - V. Lucherini, E. De Sanctis e P. Di Giacomo Frascati Report LNF-78/31 (1978).
- (31) - A. O. Komar, S. P. Kruglor and I. V. Lopator Nucl. Instr. and Meth. 82, 125 (1970).
- (32) - P. Di Giacomo e V. Lucherini Frascati Report LNF-78/8 (1978).
- (33) - E. Mancini and M. Sanzone Nucl. Instr. and Meth. 66, 87 (1968).
- (34) - S. Pasquini e A. R. Redon Frascati Report LNF-77/34 (1977).
- (35) - G. P. Capitani, E. De Sanctis, S. Pasquini e A. R. Redon Frascati Report LNF-78/2 (1978).
- (36) - E. K. Hyde: The Nuclear Properties of the Heavy Elements (Prentice-Hall, Inc., Englewood Cliffs, New Jersey, 1964) v. III cap. 13.
- (37) - V. Emma and S. Lo Nigro; Nuclear Instr. and Meth. 128, 355 (1975).
- (38) - G. Foti, J. W. Mayer and E. Rimini: in Ion. Beam Handbook for Material Analysis ed. by J. W. Mayer and E. Rimini (Academic Press, Inc. N. Y. 1977) cap. II p. 21.

CURRENT LNF PREPRINTS AND REPORTS

- LNF-79/1(P) F. Felicetti and Y. Srivastava:
RESONANT SPACE AND TIME-LIKE PION FORM FACTOR
Submitted to Phys. Lett.
- LNF-79/2(R) P. Corvisiero, F. Masulli e A. Zucchiatti:
CALCOLO DI MONTECARLO PER LA DISTRIBUZIONE DI PERCORSO DI
ELETTRONI IN NaI.
- LNF-79/3(R) E. Righi e M. Di Pofi:
IL RISCHIO DA CAMPO MAGNETICO DERIVANTE DA TECNOLOGIE
NUCLEARI: CRITERI DI PROTEZIONE SANITARIA.
- LNF-79/4(R) G. Giordano and E. Poldi Alai:
GEOMETRY OF GAUSSIAN BEAMS AND LASER CAVITIES.
- LNF-79/5(R) S. Gentile e E. Polli:
PROBLEMI DI SOFTWARE ED HARDWARE NELLA MESSA ON-LINE DI
CAMERE A FILI SU UN CALCOLATORE PDP-15.
- LNF-79/6(P) B. Touschek:
AN ANALYSIS OF STOCHASTIC COOLING
Submitted to Nuovo Cimento.
- LNF-79/8(R) A. Turrin:
OPTIMUM ROTATION ANGLE OF A SIBERIAN SNAKE.
- LNF-79/7(R) V. Bellini, E. De Sanctis, P. Di Giacomo, V. Emma, S. Gentile, C. Guaraldo,
S. Lo Nigro, V. Lucherini, C. Milone, G. S. Pappalardo and A. R. Reolon:
FISSION INDUCED IN HEAVY ELEMENTS BY THE LEALE MONOCHROMATIC
BEAM OF FRASCATI.
- LNF-79/9(P) E. Etim:
A STOCHASTIC MODEL IN MOMENTUM SPACE FOR THE EMISSION OF
INFRARED RADIATION
Submitted to Phys. Lett.
- LNF-79/10(P) E. Etim:
GENERALIZED HERMITE POLYNOMIAL EXPANSION IN THE THEORY OF
INFRARED RADIATIVE CORRECTIONS
Submitted to Math. Phys. Lett.

AVAILABLE FROM (It is not necessary to write to the authors):

Servizio Documentazione
INFN - Laboratori Nazionali
Cas. Postale 13
00044 FRASCATI (Italy) .